

# Study of Groundwater Potentiality and Sea Water Intrusion along the Coastal Plain, Wadi Thuwal, KSA- A Case Study Based on DC Resistivity

Mansour A. Al-Garni\* and Hamdy I.E. Hassanein

*Geophysics Department, Faculty of Earth Sciences, King Abdulaziz University, Saudi Arabia,  
\*Email: maalgarni@kau.edu.sa.*

<sup>2</sup> 170

(SLM)

**ABSTRACT:** The present study mainly aims to outline zones that have groundwater potentiality with good quality and those which are affected by sea water intrusion. The electrical resistivity data were acquired over an area of about 170 km<sup>2</sup> of a coastal plain, Wadi Thuwal, which is bounded by the Red Sea in the west and the volcanic hills in the east. In such an area, resistivity measurements, using n-layering model, generally reveal a wide range of resistivity values which do not reflect the reality. Hence, the statistical analysis has to be involved to overcome this problem and to make the final interpretation reliable. In our case, the n-layer models were modified to other statistical geoelectric models (SLM), consisting of a number of layers equivalent to the stratigraphic layering beneath each VES site. The modified models were used to outline the depth to the bed rock, groundwater accumulation zones and water table as well as to define the effect of sea water intrusion through the study area.

**KEYWORDS:** Wadi Thuwal; Coastal plain; DC resistivity; N-layering model; Statistical model.

## 1. Introduction

The DC- resistivity in general has been successfully used to delineate the fresh water/saline water interface (El-Waheidi, 1992; Choudhury *et al* 2001) as well as water content (Kessels *et al* 1985). The studied area is about 170 km<sup>2</sup> along the Red Sea coastal plain where it lies at the downstream of Wadi Khulase (Figure 1). It is mainly covered by Holocene Wadi deposits, Quaternary basalts (Harrat Thuwal) and Miocene sediments. It is shown that the structural pattern beneath the study area is affected by more than one phase of faulting. The surface of Miocene deposits is considered as a bed rock (M. Abdulwahid unpublished data). The lithology and configuration of the surface of Miocene deposits play the main significant role in building up the drainage pattern beneath the eolian and alluvian cover of the study area.

This work represents an attempt to study the subsurface structural setting and to delineate the ground water distribution in Wadi Thuwal area, as well as the seawater intrusion effect through it.

## 2. Data acquisition

A vertical electrical sounding (VES) survey was conducted at 88 selected sites using Schlumberger array to measure the surface and subsurface variation in resistivity. The well-known ELREC-T system (IRES) was used as an electrical resistivity meter, utilizing 1200 kW.

### 2.1 Vertical electrical sounding data analysis

#### 2.2.1 N-layering technique

A VES survey provides a series of apparent resistivity values as a function of depths. These values are obtained at each VES location, using different electrode spacings. The half current electrode spacing ( $AB/2$ ) reached up to 140 m where the spacing between the potential electrodes (MN) varied from 2m to 20m according to the rule of thumb of Schlumberger array ( $AB \geq 5MN$ ). These measurements were made along 8 E-W profiles, covering the study area. The resistivity curves fall into the following types: QH, KQ, HK, Q and H. Sampling of the continuous smoothed curve at the rate of 6 logarithmically equally spaced points per logarithmic cycle was done to obtain a digitized sounding curve. In general, sampling the apparent resistivity is done from right to left, starting from the largest current electrode spacing, where the effect of near surface inhomogeneity is disregarded (Al-Garni, 1996). We used Zohdy's method (Zohdy, 1989) to invert the VES field resistivity measurements to a number of horizontal geoelectric layers.

The study area has a large aerial extension with significant variable surface and subsurface structural and environmental depositional regimes built up over a long period of time, where these two factors have led to a wide range of resistivity values (0.9-2568.5 ohm.m). Therefore, statistical analysis was suggested to define and classify the obtained resistivity data as normal distribution groups with known statistical parameters related to certain lithological and/or structural environment units and constrained by reliable depth limits.

#### 2.2.2 Statistical analysis

The process of statistical analysis involves all the data as one population to check their normality. The standard deviation of the measured resistivity values all over the area is 227. The Kolmogorov-Smirnov test of normality (Clark and Evans, 1954; Montgomery and Runger, 1994; Cressie, N.A.C, 1991; and King, Ronald S. and Bryant Julstrom 1982) shows that this population of resistivity measurements do not have a normal distribution, where the Kolmogrov-Smirnov statistical index  $\gg$  the critical value (Table 1). This indicates that the population of data assemblage could be classified into different populations; hence, the statistical analysis was used to implement the classification.

# STUDY OF GROUND WATER POTENTIALITY AND SEA WATER INTRUSION

Table 1. Results of statistical analysis of the resistivity data of the study area.

# of data	Min	Max	mean	S.D.	K-S	C.K-S at $\alpha=.05$
761	0.86	2568.5	127.8	227	0.288	0.049

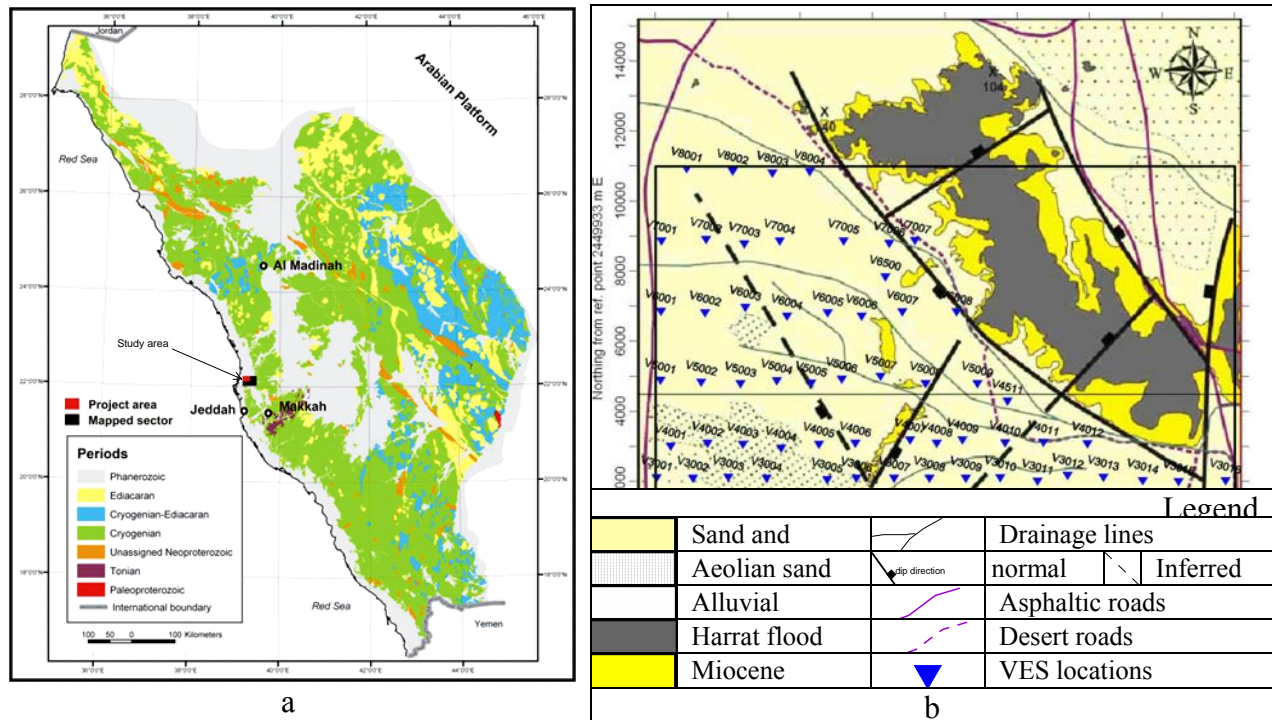


Figure 1. Location (a) and Geology and the VES sites distribution of Wadi Thuwal area, KSA (Al-Garni *et al* 2009) (b).

Accordingly, the calculated resistivity values, using n-layering modeling technique, are classified into six different normal distribution classes each of which corresponds to certain lithological ensembles of distinguishable resistivity character. Table 2 shows the statistical parameters and the results of normality distribution analysis. To define the depth limitations of each one of the classes, the data involved in each class was plotted individually and compiled as a depth resistivity graph (Figure 2), which shows that the resistivity values decrease with increasing depth. The upper 10 m, which is related to the surface and near surface lithological variations, has a wide resistivity range (1-2570 ohm.m). The resistivity of the section between 10 and 20 m ranges between 0.8 -200 ohm.m. It is underlain by the third section (20-30 m), with resistivity values, ranging between 1.8-40.0 ohm.m. The last section, which is deeper than 30 m, has a resistivity range between 2.5-20 ohm.m.

The geoelectric n-layering model (NLM), which was obtained from the n-layer modeling technique (Zohdy, 1989), can be modified to another equivalent geoelectric statistical layering model (SLM). In this case, the number of geoelectric layers will be reduced and it will lead to more realistic lithological units. For example, at VES 1001, ten layers are interpreted using n-layer technique (NLM) whereas this number is reduced to six geoelectric layers using statistical analysis (SLM).

Table 2. Results of normality test and the 6 unit statistical parameters.

Statistical parameters	Code number					
	1	2	3	4	5	6
Number of values	194	151	134	168	104	10
range	0.9-	8.1-24.7	25.2-78.6	80.8-255.3	260.2-933.3	960.3-2568.5
Mean	4.1	14.2	45.7	149.6	478.9	1322.4
Standard deviation	1.9	4.8	16.1	52.3	186.3	482.4
Kolmogorov-Smirnov stat. index	0.096	0.105	0.107	0.102	0.129	0.253
Critical K-S stat, pha =.05	0.097	0.109	0.116	0.104	0.132	0.409

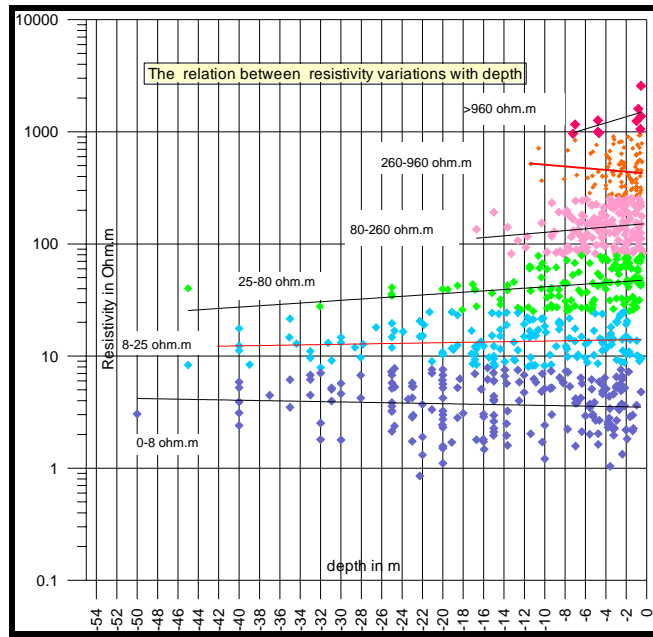


Figure 2. Resistivity clusters versus depths.

The developed classification, resistivity contours, and the geology are superimposed all together to implement the correlation (Figure 3). This shows certain distinctive zones of low resistivity values, taking an elongated extension, which is mostly attributed to the surface courses of the floods during the successive rainy seasons. The interpreted low resistivity values, using statistical geoelectric layers (SGL) (1, 2 and 3), are present on the surface of such zones. The interpreted higher resistivity values, using SGL (4, 5 and 6), occur mainly in areas that are covered by alluvial terraces.

The interpreted depth beneath each model was reduced to sea level in order to reveal the relation between the resistivity distributions and the geomorphologic and environmental variations. The obtained resistivity values and their corresponding depths were used to construct eight W-E cross-sections along profiles, coded as 1000,

## STUDY OF GROUND WATER POTENTIALITY AND SEA WATER INTRUSION

2000, 3000, 4000, 5000, 6000, 7000 and 8000, respectively (Figure 4). The interpreted resistivity classes (Table 2) were considered as contour intervals.

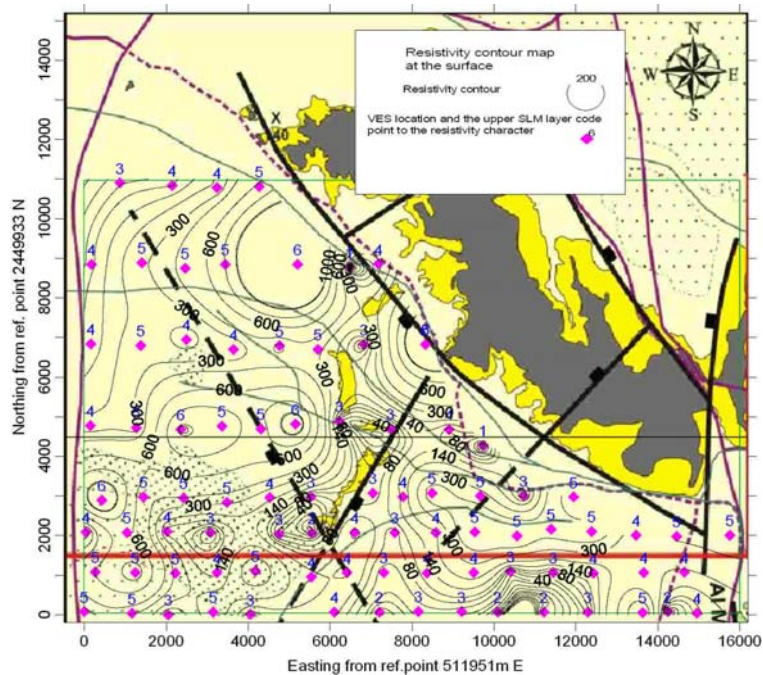


Figure 3. Distribution of SGL, surface resistivity contours, and geology of Wadi Thuwal area.

### 3. Interpretation of the resistivity data

The lateral and vertical resistivity variations along each profile show that the basement rocks and the overlain sedimentary Miocene deposits were affected by different structural events, changing their structural setting at the surface of the bedrock. Hence, the depositional and hydrological regimes of the recent Quaternary deposits are controlled by these changes. (Figure 4) shows that the main water table level of the study area is the sea level, ranging between 10 and 20 m from the surface. The bedrock is characterized by low resistivity values (1 to 8 ohm.m), extending beneath the entire study area. This indicates that the lithological composition of the bedrock is mainly clay, which may be attributed to the salinity content near the shoreline (at the north western part of the study area, Figure 6).

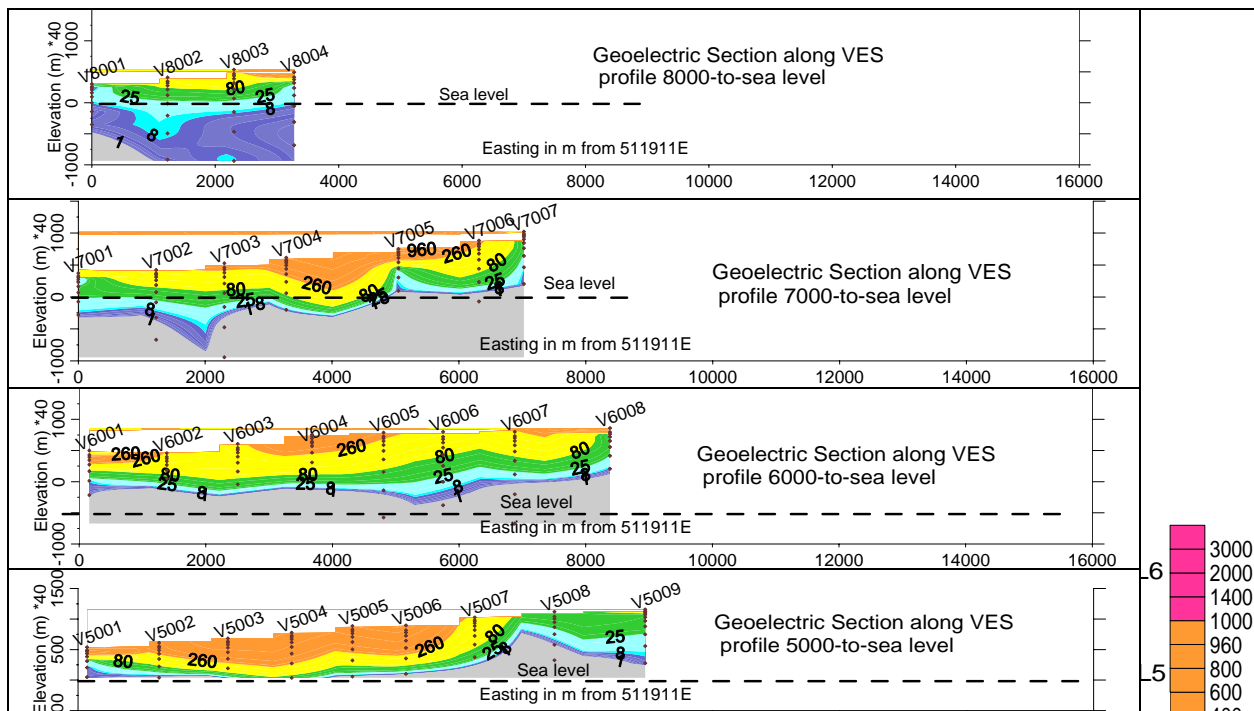
The bedrock is overlain by two geoelectric layers. The first, coded No.2, ranging between 8 and 25 ohm.m in resistivity, represents sediments of sand and gravel saturated with water regardless of the quality. The second, coded No.3, which ranges in resistivity between 25 and 80 ohm.m, represents sediments of sand and gravel partially saturated with water (Figure 4). These two units are considered to be the most significant units for conducting groundwater exploration, where the thickness of water saturation of these zones varies according to the level of precipitation. The resistivity behavior of unit No.3 is almost the same as that of No.2, yet the thickness of the water saturation zone is greater. These two zones can be observed along profiles 2000 (V2007 and 2014), 3000 (V3006, 3008, 3014 and 3015), 4000 (between V4008 and 4011), 5000 (V5008 and 5009), 6000 (V6005 and 6006), 7000 (V7003) and 8000 (V8002) (Figure 4).

The three geo-electric units No. 4, 5 and 6 are present frequently, occupying the upper part of the geo-electric sections, and they are characterized by high resistivity values. These units have no significant impact on the water exploration. However, their lithological characters may control the flow of the floods and water percolation through them.

Figures (5a and b) show the topographic contour maps (depth to sea level) of the upper surface of both geo-electric units No.1 and 2, respectively, which reveal the effect of the structural events. There are five zones (SZ1, SZ2, SZ3, SZ4, and SZ5) of low resistivity values, which can be delineated based on the correlation between the resistivity and bedrock topography (Figure 5a). Three zones (SZ1, SZ2 and SZ3), which are located below sea level, are invaded by the sea water intrusion where high salinity of groundwater is expected. The other two zones (SZ4 and SZ5), which are located above sea level, prevalently contain an abundance of clay accumulations.

Figure (5b) shows five significant catchment zones (Z1, Z2, Z3, Z4 and Z5) within the second geo-electric layer. The resistivity values of this layer and its relative topography (above the sea level) indicate the presence of water of good quality. Figure (5c) shows the thickness variations of this layer all over the studied area, where the average thickness of the groundwater bearing layer at these zones is about 10 m.

Figure (6) shows the interpreted faults and outlines the sea water intrusion zones (SWI) and fresh water occurrences (FWO-1, FWO-2, FWO-3 and FWO-4). It shows also that the sea water intrusion and fresh water flow are controlled by the subsurface structures. The area at the east of the fault F4 is affected by sea water intrusion, whereas the most expected fresh water occurrences are located at the west of F7.



Figures to be completed on the next page.



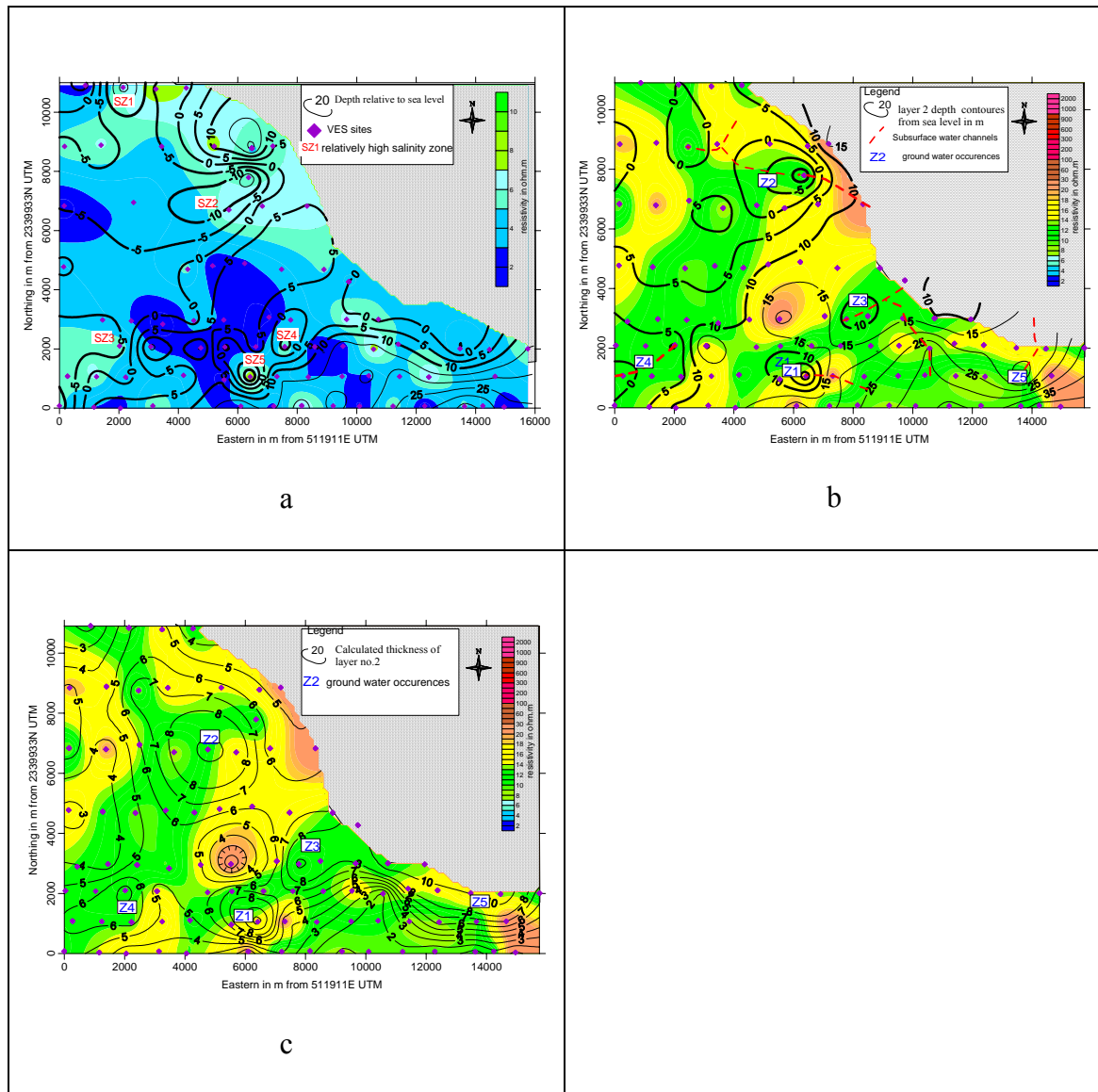


Figure 5. The depth contour map of the upper surface of the interpreted SGL no.1 (a), the depth contour map of the interpreted SGL no. 2 (b), and thickness contour map of layer no. 2, showing zones of water of relatively good quality (c).

# STUDY OF GROUND WATER POTENTIALITY AND SEA WATER INTRUSION

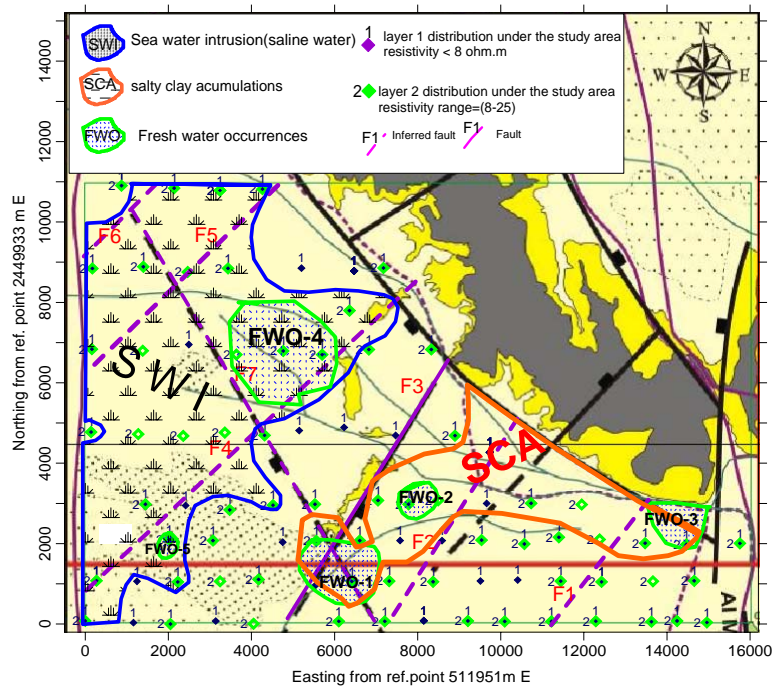


Figure 6. Interpretation results of Wadi Thuwal area.

## 5. Acknowledgment

The authors are greatly thankful to the King Abdulaziz City for Science and Technology (KACST) for supporting this study AT-26-82. The authors would like to express their sincere thanks to the editors and the anonymous reviewers, for the thorough review that highly improved the original manuscript.

## 6. References

- ABDULWAHID, M. (unpublished data), Geology and structural framework of Harrat Thuwal, North of Jeddah, Saudi Arabia.
- AL-GARNI, M.A. 1996. Direct current resistivity investigation of groundwater in the lower Mesilla Valley, New Mexico and Texas: MS thesis, Colorado School of Mines, 120 p.
- AL-GARNI, M.A., EL-BEHIRY, M.G, GOBASHY, M.M, HASSANEIN, H.I., and EL-KALIOUBY, H.M. 2009. Geophysical studies to assess groundwater potentiality and quality at Wadi Thuwal area, North of Jeddah, KSA. *King Abdulaziz City for Science and Technology*, project No. At-26-82, p. 394.
- CHOUDHURY, K., SAHA, D.K., and CHAKRABORTY, P. 2001. Geophysical study for saline water intrusion in a coastal alluvial terrain. *J. Applied Geophy.*, **46**: 189-200.
- CLARK, P. AND EVANS F. 1954. Distance to nearest neighbor as a measure of spatial relationships in populations. *Ecology*, **35**: 445-453.
- CRESSIE, N. A. C. 1991. *Statistics for Spatial Data*. John Wiley & Sons Inc., New York.

- EL-WAHEIDI, M.M., MERLANTI, F., and PAVAN, M. 1992. Geoelectrical resistivity survey of the central part of Azraq plain (Jordan) for indentifying saltwater/freshwater interface. *J. Applied Geophy.*, **29**: 125-133.
- KESSELS, W., FLENTGEH, I., KOLDITZ, H. 1985. DC geoelectric sounding to determine water content in the salt mine asse (FRG). *Geophysical Prospecting*, **33**: 456-446.
- KING, RONALD S. and BRYANT JULSTROM. 1982. *Applied Statistics Using the Computer*. Alfred Publishing Company, Sherman Oaks, California.
- Montgomery, D.C. and Runger G.C. 1994. *Applied Statistics and Probability for Engineers*. John Wiley & Sons Inc., New York.
- ZOHDY. A.A.R. 1989. A new method for the automatic interpretation of Schlumberger and Wenner sounding curves. *Geophysics*, **54**: 245-253.
- 

Received 25 May 2009  
Accepted 21 April 2010